IVR in Overtones of the Acetylenic C-H Stretch in Propyne

Aseem Mehta, A. A. Stuchebrukhov,† and R. A. Marcus*

Arthur Amos Noyes Laboratory of Chemical Physics,‡ 127-72, California Institute of Technology, Pasadena, California 91125

Received: October 4, 1994; In Final Form: November 29, 19948

Quantum calculations are reported for the high-resolution spectra and dynamics of the first and second overtone of the acetylenic C-H stretch (ν_1) in propyne. The calculational method used is similar to that we have used earlier for lower energy states. Lack of low-order Fermi resonances lead to a vibrational superexchange mechanism of decay of the initially populated bright state. The importance of the total density of states and quartic couplings between zeroth-order states is investigated. Comparison with recent experimental results is discussed.

I. Introduction

In previous papers^{1,2} we considered the vibrational spectrum and the corresponding intramolecular vibrational relaxation (IVR) of the fundamental and first overtone excitations of the acetylenic C-H stretch in (CX₃)₃YCCH molecules using a tierstructure formalism. In one of the articles,2 analysis of an approximate molecular Hamiltonian for the acetylenic stretch fundamental excitation in (CH₃)₃CCCH provided a Lorentzianlike line shape, with a fwhm (full width at half-maximum) equal to 0.03 cm⁻¹, in agreement with experimental results. The Fourier transform of the calculated spectrum corresponded to a slow but statistical decay occurring out of the acetylenic stretch fundamental excitation on a time scale of ≈200 ps. The slowness of this decay time might have been considered surprising due to the fact that the density of states for this molecule at the given energy is high.3 Within the tier formalism with cubic anharmonic couplings in normal coordinates between states in adjacent tiers, the slowness of the relaxation (narrowness of the spectrum) was found to be due to a lack of direct low-order Fermi resonances, leading to a vibrational superexchange (or dynamical tunnelling) mechanism. In the latter the bright state decays into a degenerate vibrational quasicontinuum, mediated by off-resonant virtual transitions. As described in refs 1 and 2, this mechanism may be understood in terms of a tunnelling of trajectories in phase space through a dynamical barrier. In the spectroscopic description, the extensively offresonant nature of the states directly coupled to the bright state leads to a narrow spectral line.

In the present paper, the methods described in these articles are applied to overtone states in a smaller molecule, propyne (H₃CCCH), prompted by recent experiments.^{4,5} Excitations involving the acetylenic C-H (ν_1) stretching modes were studied. The bands analyzed are $2\nu_1$ and $3\nu_1$.

Experimentally, Lehmann, Scoles, and co-workers have investigated the latter of these two bands in a study to explore the spectroscopic differences of nearly pure state $3\nu_1$ and the combination mode $\nu_1 + 2\nu_6$ that has energy already partly distributed.⁴ The high-resolution spectra of these bands, incorporating the details of the splitting of a single line due to anharmonic interactions, indicated, in a temporal description, that the rate of relaxation of the $3\nu_1$ state is faster. The difference in the density of states was not considered to be large enough to explain the anomaly, the $3\nu_1$ and $\nu_1 + 2\nu_6$ states

being close in energy. The $3\nu_1$ (J'=0) state, in a narrow spectral range of 0.1 cm⁻¹ studied experimentally, showed several lines, while the $\nu_1 + 2\nu_6$ state in a similar spectral range showed only one line.

Perry and co-workers have investigated the $2\nu_1$ and the nearly isoenergetic $\nu_1 + \nu_6$ bands⁵ and found that the spectra of individual J, K states are split. For low K states the splitting is small and the spectrum in each case consists of one major peak surrounded by a few small peaks, each of which has an amplitude of less than 10% of the main peak. The available data hints at a larger number of perturbers for the pure overtone $2\nu_1$ than for the $\nu_1 + \nu_6$ band. In the present paper we present the results for the $2\nu_1$ and the $3\nu_1$ bands.

For the calculated relaxation, our analysis yields a behavior of the $2\nu_1$ and $3\nu_1$ states that follows a vibrational superexchange mechanism, due to the lack of low-order Fermi resonances. The decay is governed, thereby, by the few directly coupled off-resonant states that provide virtual couplings.

The calculated IVR characteristics are quite different at the two energy scales. At the lower energy, about 6000 cm⁻¹, we find the beginnings of some perturbations to the regular spectra due to interactions with bath states. However, the energy is still mainly localized in the bright state. On the other hand, at about 9500 cm⁻¹, there are available to the bright state a large enough number of quasi-resonant states such that real statistical IVR can occur leading to irreversible decay (modulated by some quantum beats) of population out of the bright state.

II. Tier Model

The tier model has been described elsewhere.¹ The Hamiltonian is written in normal mode coordinates as

$$H = \frac{1}{2} \sum_{i} \omega_{i} (q_{i}^{2} + p_{i}^{2}) + \frac{1}{3!} \sum_{i,j,k} \phi_{ijk} q_{i} q_{j} q_{k} + \frac{1}{4!} \sum_{i,j,k,l} \phi_{ijkl} q_{i} q_{j} q_{k} q_{l} + \dots$$
(1)

The energy of each of the zeroth-order states in the basis set is calculated using the expression⁶

$$E(v_1, v_2, ..., v_n) - E_{\text{ZPE}} = \sum_{i} \omega_i v_i + \sum_{i} \sum_{k>i} x_{ik} \left(v_i v_k + \frac{v_k d_i}{2} + \frac{v_i d_k}{2} \right)$$
(2)

where d_i is the degeneracy of the *i*th mode. The intermode coupling is due to nondiagonal anharmonic terms in eq 1.

 $^{^\}dagger$ Permanent address: Department of Chemistry, University of California, Davis, CA 95616.

[‡] Contribution No. 8991.

^{*} Abstract published in Advance ACS Abstracts, February 1, 1995.

TABLE 1: Limited Number of Cubic and Quartic Force Constants in Internal Coordinates for Propyne Included in the Nonlinear Transformation into Normal Coordinates^a

| ijk | f_{ijk} | ref | ijkl | f_{ijkl} | ref |
|-------------------|-----------|-----|----------------------------|------------|-----|
| $S_5S_5S_5$ | -38.35 | 10 | $S_5S_5S_5S_5$ | 196.0 | 10 |
| $S_4S_4S_4$ | -109.23 | 10 | $S_4S_4S_4S_4$ | 536.2 | 10 |
| $S_5S_5S_4$ | 0.40 | 10 | $S_5S_5S_4S_4$ | -1.287 | 10 |
| $S_5S_4S_4$ | -0.193 | 10 | $S_5S_5S_5S_4$ | -2.663 | 10 |
| $S_5S_{10}S_{10}$ | -0.202 | 10 | $S_5S_4S_4S_4$ | -0.675 | 10 |
| $S_4S_{10}S_{10}$ | -0.802 | 10 | $S_5S_5S_{10}S_{10}$ | 0.242 | 10 |
| $S_3S_3S_3$ | -26.50 | 11 | $S_5S_4S_{10}S_{10}$ | -0.025 | 10 |
| $S_1S_1S_1$ | -18.67 | 12 | $S_4S_4S_{10}S_{10}$ | 0.137 | 10 |
| $S_6S_6S_6$ | -12.70 | 12 | $S_{10}S_{10}S_{10}S_{10}$ | 1.752 | 10 |
| $S_1S_7S_7$ | -0.33 | 12 | $S_1S_1S_1S_1$ | 50.0 | 12 |
| $S_6S_7S_7$ | -0.29 | 12 | $S_6S_6S_6S_6$ | 75.0 | 12 |
| $S_7S_7S_7$ | -0.18 | 12 | $S_1S_1S_6S_6$ | 52.0 | 12 |
| $S_1S_6S_6$ | -16.56 | 12 | $S_1S_6S_6S_6$ | 37.0 | 12 |

 a S_i are symmetric internal coordinates as defined by Duncan in ref. 9. Force constants are in Å rad units.

The nondiagonal anharmonicity terms $q_iq_jq_k$ couple different zeroth-order states in the Hamiltonian and are written in terms of creation and annihilation operators. Starting with the bright state, and with the ϕ_{ijk} values available, the $q_iq_jq_k$ operators are used to generate states in further tiers. The states are kept within specified energy windows, and they are accepted or rejected on the basis of an artificial intelligence (AI) search method. This search method is used to select the states that are important in the relaxation while keeping the problem computationally tractable. States that are highly detuned in energy from the bright state or are coupled with a small matrix element do not contribute to the relaxation and are discarded during the AI search using an evaluation function that has been described in ref 1.

The anharmonic constants ϕ_{ijk} in eq 1 are obtained by the transformation of empirical force fields in internal coordinates⁷ into normal coordinates. These empirical force constants (in internal coordinates) are transformed nonlinearly into normal coordinates using the software package due to Handy and coworkers (SPECTRO).⁸

The empirical anharmonic force field used for these calculations is the quartic force field in internal symmetry coordinates from refs 9-12. The quadratic part of the force field from ref 9 was fit to some approximations of the harmonic frequencies $(\omega_i$'s) rather than the energies of the fundamental transitions. The quadratic force field and the most important (and available) cubic and quartic force constants (Table 1) were used as input into the routine SPECTRO. The latter nonlinearly transforms the internal coordinate force field into a normal coordinate force field and calculates, by a perturbation theory expression, the (3N-6)(3N-6) anharmonic constant matrix x_{ij} . These constants are used to calculate the energy of each state in eq 2. The calculated ϕ_{iik} values are used to evaluate the coupling terms between zeroth-order states in adjacent tiers. We note again that the wave functions of the zeroth-order states were those of a multidimensional harmonic oscillator, but their energies were corrected using eq 2.

A Morse oscillator function for the C-H acetylenic stretch has also been used by some investigators in their calculations. We calculated the matrix elements between zeroth-order states using Morse wave function selection rules and found that even at the $3\nu_1$ level (9500 cm⁻¹; $D_e(\equiv C-H) \approx 35\,000$ cm⁻¹) the zeroth-order wave function can be well approximated by a harmonic oscillator without the introduction of significant error ($\leq 10\%$, typically). Therefore, all the calculations reported used harmonic oscillator basis functions. The energies of the zeroth-order states were however, obtained from eq 2.

Due to the tractable size of the molecule, an ab initio calculation of propyne was also performed with Gaussian 92.¹³ This calculation, with a 6-31G* basis set at the restricted Hartree-Fock level, generated quadratic and cubic force constants in Cartesian coordinates. These constants were transformed linearly into the normal-coordinate-based ϕ_{iik} values. The latter were, in turn, used to couple the harmonic oscillator zeroth-order states. The cubic force constants obtained from ab initio calculations are complete at the given level of theory and can be used as an approximate test of the force field in internal coordinates that (at cubic and higher levels) had been cobbled together from various sources. The latter piecedtogether force field is necessarily incomplete since all the cubic internal coordinate force constants are not known. The ab initio force field was used only as a qualitative check on the empirical force field. The results presented in this paper are all from the empirical force field.

Due to the higher energy $(E(\mathbf{v})-E_{ZPE}\approx 6000 \text{ or } 9000 \text{ cm}^{-1})$ of the states analyzed, when compared with our study of the fundamental stretch in $(CH_3)_3CCCH$ $(E(\mathbf{v})-E_{ZPE}\approx 3000 \text{ cm}^{-1})$, we have found that some quartic couplings have to be included if the model is to realistically model the actual physical process. This point is elaborated upon later. There are numerous unknown or only crudely estimatable quartic force constants ϕ_{ijkl} . We have included their effect in the tier structure in an approximate way by assigning a coupling element, chosen as indicated below, to the coupling of states $|i\rangle$ and $|j\rangle$ in tiers differing by two (e.g., tier n and tier n+2) if the quantity η_{ij} , defined by

$$\eta_{ij} = \sum_{k} |\nu_k^i - \nu_k^j| \tag{3}$$

is less than or equal to 4. Here, v_k^i is the number of quanta in the kth oscillator of the ith state.

It should be the noted that the terms coupling states in adjacent tiers (also referred to as matrix elements since they are the off-diagonal terms in the vibrational Hamiltonian) differ from the matrix element term used in some of the experimental papers. The latter arise in the Lawrance–Knight¹⁴ deconvolutions of spectra and are approximately related to the superexchange matrix element $\langle 0|V|k\rangle$ in the present formalism via a perturbation-theory-based expression such as

$$\langle 0|V|k\rangle \sim V_{01} \frac{V_{12}}{\Delta E_{12}} ... \frac{V_{k-1,k}}{\Delta E_{k-1,k}}$$
 (4)

there being a sum over the various superexchange paths connecting $|0\rangle$ and $|k\rangle$. There is, of course, a large difference in the magnitude between the superexchange "matrix elements" $\langle 0|V|k\rangle$ when compared with the values of V_{01} , V_{12} , etc.

The importance of including a final tier with a high density of states (when a high density of states exists for the given molecule at the energy in question as in propyne at 9000 cm⁻¹), so as to approximate the real total density of states of the dark states, was established in ref 2. We make the same addition here in the calculations. The total number of added states that model the quasi-continuum vary from 600 to 1000 in an energy window of 3-5 cm⁻¹, such that the total density of states is approximately 200/cm⁻¹. The latter is slightly higher than the density of states estimated for propyne (150/cm⁻¹) with the correct symmetry at the specified energy (≈9000 cm⁻¹). The slightly higher value is used because the interaction of the states in the finite final tier with the previous tiers leads to the repulsion of some of the final tier states into a larger window. The matrix element with which these final tier states are coupled to states

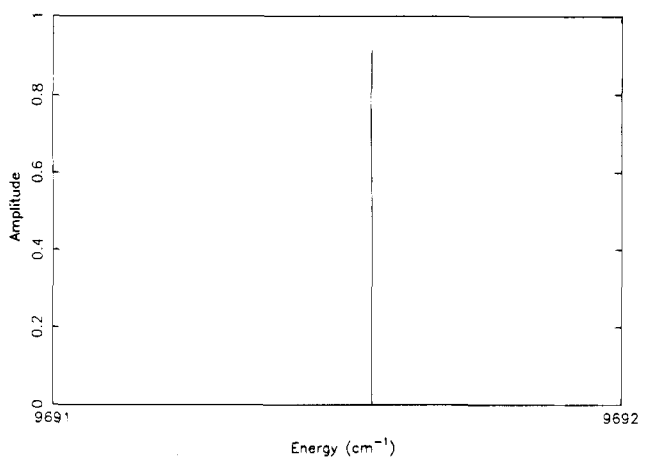


Figure 1. Spectrum corresponding to the $3\nu_1$ band for CH₃CCH. No quartic couplings or final tier of dense states is added.

in the previous tier is estimated from the average cubic coupling between states in previous tiers. Each state in the final tier is coupled to a single state in the previous tier.

The states in the final tier are placed randomly, and the robustness of the calculation with respect to this random placement and to the approximate magnitudes of the quartic coupling values is explored below, where some typical results are given.

III. Results

3.1. 3v₁. a. No Quasi-Continuum. With the above algorithm for generating the sequentially coupled model with a given bright state, the tier structure was generated with the bright state containing three quanta of energy in the acetylenic C-H stretch. The pure normal mode wave function of the zeroth-order bright state is denoted by $|\phi_0\rangle$, with its energy having been corrected using eq 2. Experimentally, about five peaks were observed in an energy window of approximately 0.1 cm⁻¹ (for J' = 0). This number corresponds to at least a minimum of 50 states/cm⁻¹ coupled well with the bright state, since some peaks may have been in the signal/noise background and so not observed. This density of states of 50/cm⁻¹ is on the same order as the calculated total density of vibrational states (150/cm⁻¹) with the correct symmetry.4 Using the previously described AI search method, a total of 1048 "well-coupled" states in 10 tiers were selected within a large energy window of 500 cm⁻¹ for each tier. Diagonalization of this vibrational Hamiltonian with only cubic couplings resulted in a spectrum,

$$I(\omega) = \sum_{i} |\langle \psi^{\text{init}} | \mu | \psi_{i} \rangle|^{2} \delta(\omega - E_{i})$$

$$= \sum_{i} |\langle \psi^{\text{init}} | \mu | \phi_{0} \rangle|^{2} |\langle \phi_{0} | \psi_{i} \rangle|^{2} \delta(\omega - E_{i})$$

$$= c \sum_{i} |\langle \phi_{0} | \psi_{i} \rangle|^{2} \delta(\omega - E_{i})$$
(5)

dominated by only one peak (Figure 1), for which $\langle \phi_0 | \psi_i \rangle^2 \approx 0.9$, for some *i*. Here the $|\psi_i\rangle$ form a complete set of eigenfunctions and *c* is a constant. In deriving eq 5, we have assumed that there is only one zeroth-order state, $|\phi_0\rangle$ (the bright state), that has a nonzero matrix element of the type $\langle \phi_0 | \mu | \psi^{\text{init}} \rangle$, where μ is the dipole moment operator and $|\psi^{\text{init}}\rangle$ is the initial vibrational state (experimentally, it had one quantum in ν_1).

b. Quasi-Continuum Added. To simulate the presence of the high density of nearly degenerate states that are well separated in phase space from the bright state, a single, dense tier of quasi-degenerate states was then added to the final (here,

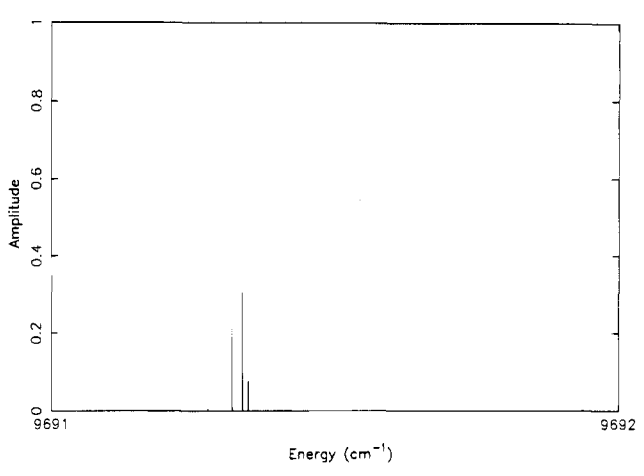


Figure 2. Spectrum corresponding to the $3\nu_1$ band for CH₃CCH showing the transformation (from Figure 1) due to the final tier of resonant states and quartic couplings.

tenth) tier with a density of states such that the total density of states approximates the actual value. One thousand states, randomly placed in a window of size 5 cm⁻¹, were coupled to states in the tenth tier with matrix elements estimated from the average matrix elements in previous tiers. This addition of a quasicontinuum yielded no observable change in the spectrum, *i.e.* yielded a spectrum similar to Figure 1.

- c. Addition of Quartic Terms. Upon the inclusion of small quartic terms that couple the states in the manner described above (by the calculation of η_{ij}) and without the addition of the final dense tier of states, the amplitude of the major peak diminished slightly (to 0.75), with the remaining amplitude being distributed over spectral lines in a large energy range ($\approx 100 \, \mathrm{cm}^{-1}$). When the final tier of states was added to this cubicand quartic-coupled Hamiltonian, the spectrum was transformed from one where there is a single dominant peak to a more fractionated type (Figure 2). The single peak of previous calculations split into a few (three to six) "major" peaks within an energy range of $0.07-0.15 \, \mathrm{cm}^{-1}$. The details of the calculated spectrum, however, depended upon the particular random choice of the energies and the coupling terms of the states in the final tier.
- d. Time-Dependent Behavior. It is useful to compare the autocorrelation functions of the spectra (survival probability $p_0(t)$ of the bright state) with and without the extra tier present and with and without quartic couplings:

$$p_{o}(t) = |\langle \phi_{0} | \phi(t) \rangle|^{2}$$

$$= |\sum_{i}^{N} |\langle \phi_{0} | \psi_{i} \rangle|^{2} e^{-iE_{i}t}|^{2}$$
(6)

where $\phi(t)$ is the wave function at time t which evolves from ϕ_0 ($p_0(0)$ is unity). The right-hand side of eq 6 is proportional to $|\int_{-\infty}^{\infty} I(\omega) e^{-i\omega t} dt|^2$, where $I(\omega)$ is given by eq 5. As indicated by the spectrum (which is dominated by a single peak of ≈ 0.9 , of which the autocorrelation function is the Fourier transform), $p_0(t)$ remains constant for a time of up to 1 ns at a high value (0.8-0.9) when only cubic couplings are utilized. The same type of result is obtained upon the addition of the final dense tier of states. With the inclusion of quartic couplings but without the extra tier, the survival probability shows instead a rapid oscillatory decay to ≈ 0.6 on a femtosecond time scale (Figure 3), because of the few well-coupled nonresonant states in the initial tiers, due to direct cubic and quartic couplings. It then remains highly oscillatory and, on average, constant.

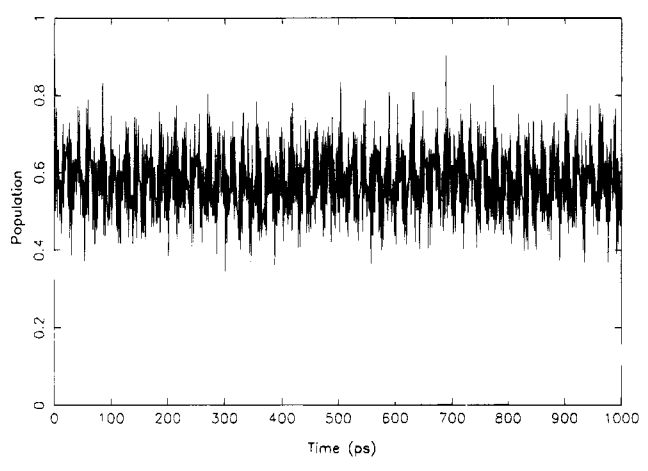


Figure 3. Survival probability (of the bright state) when quartic couplings are utilized without the final tier.

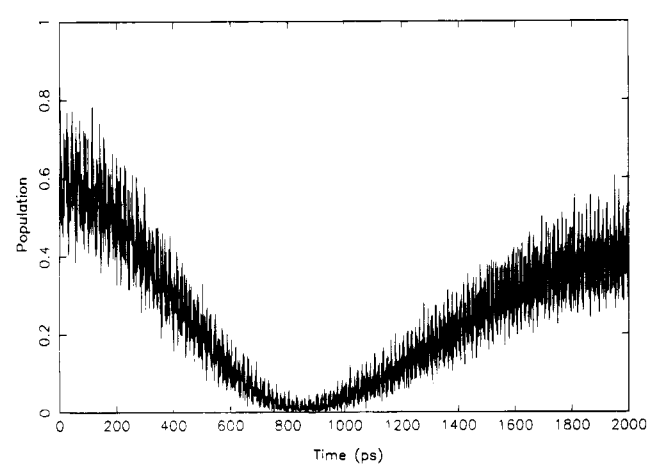


Figure 4. Survival probability corresponding to spectrum in Figure 2.

Upon the addition of the extra tier to simulate the actual presence of the quasi-continuum, the high-frequency oscillatory behavior is accompanied by smooth decay of the population into the quasi-continuum (Figure 4). The time scale of this decay is a few (two to six) hundreds of picoseconds.

Dynamically, therefore, the addition of the quartic couplings, but no quasi-continuum, changes the autocorrelation function from essentially no decay into one where there is fast femto-second time scale decay of the autocorrelation function to about ≈ 0.6 , which then, on average, remains constant but is accompanied by a large number of high-frequency components. Addition of the final tier of dense states causes real decay to occur. This finding confirms our previous conclusion that the fine structure and the irreversible relaxation of the first several overtones are due to the very high-order superexchange anharmonic couplings.

From the spectral viewpoint, the high-frequency components of the autocorrelation function, which dominate the subpicosecond dynamics, appear as small peaks far detuned from the main peak. These spectral components that are detuned from the main peak appear due to the presence of a few nonresonant states in the initial tiers that are well coupled to the bright state, which also cause the subpicosecond decay of the autocorrelation function to ≈ 0.6 . Experimentally, they might be very difficult to resolve due to their large distance from the main peaks as well as signal-to-noise limitations. There is, however, no reason for them not to occur. The smooth but not single-exponential decay appears spectrally as the splitting of the main peak into a few reasonably strong peaks within a small energy window.

e. Robustness of the Calculation. We have examined the robustness of the calculation. The quartic coupling constants were added as a random coupling between 0 and some approximate maximum value. In the final dense tier of states, the energies of the states were random within a given energy window. The matrix elements coupling states in the final dense tier with the previous tier were also random between 0 and various maximum values ($V_{\text{max}} = 5-30 \text{ cm}^{-1}$). In Figure 5, results are presented from simulations with different random realizations of these values. The figure shows that while the details of each calculation may differ, the physically relevant picture of splitting of the main peak into a few peaks within an energy range of about 0.1 cm⁻¹ remains unchanged. In Table 2, we present some statistics about each of the five spectra that have been presented in Figures 2 and 5. The numbers presented are quite representative. The quantity Γ in Table 2 is defined

$$\Gamma^2 = \frac{\sum_{i} p_i (\nu_i - \bar{\nu})^2}{\sum_{i} p_i} \tag{7}$$

where $\bar{\nu} = \sum_i p_i \nu_i / \sum_i p_i$, and $p_i = |\langle \phi_0 | \psi_i \rangle|^2$. These statistics have been calculated not over the whole spectrum (in which case the denominator in eq 7 would have been unity) but over a small window that includes just the main clump of peaks in the figures. Also in Table 2, we present the number of major components in the spectra, where a component is considered major if $|\langle \phi_0 | \psi_i \rangle|^2 \ge 0.005$, which is about 1-2% of the major peak. The window in Table 2 refers to the energy range in which these major components occur.

These results are qualitatively similar when the statistics of different spectra are compared but there is enough scatter in the data that no quantitative judgements can be made. Γ can be considered to be a rough estimate of the discrete counterpart of the fwhm and the calculated values of a few hundred megahertz are in agreement with experimental values for such molecules.³

3.2. $2v_1$. The Hamiltonian matrix of the tier structure was generated utilizing the algorithm described above. The energy window for each of the 10 tiers is 500 cm⁻¹, and 437 wellcoupled zeroth-order states form the basis set. Diagonalization of this Hamiltonian matrix with only cubic couplings resulted in a spectrum for which the amplitude of one of the peaks was greater than 0.999. Upon relaxing the AI criterion for state selection, a larger Hamiltonian matrix with 1317 basis set states was also analyzed with no change in the spectrum. This result indicates that the scheme of selecting only the most important states has captured all the physically relevant details of the spectrum as far as the cubic couplings are concerned. The complete dominance of a single peak in the spectrum shows that there is no interaction of the bright state with the bath states in the cubic Hamiltonian. Upon the addition of small phenomenological quartic couplings between states separated by one tier as described above and the addition of a final tier of states with the appropriate density of states we find that the main peak split slightly. However, the spectrum was still dominated by a single peak that had an amplitude of 0.9. The rest of the amplitude was distributed in weak daughter peaks around the main peak. Also, there were some peaks detuned more than a tenth of a wavenumber due to the direct quartic couplings. In Figure 6 we give a typical example of the slight splitting that occurs due to the quartic couplings and the final tier (note the considerably expanded, logarithmic, scale).

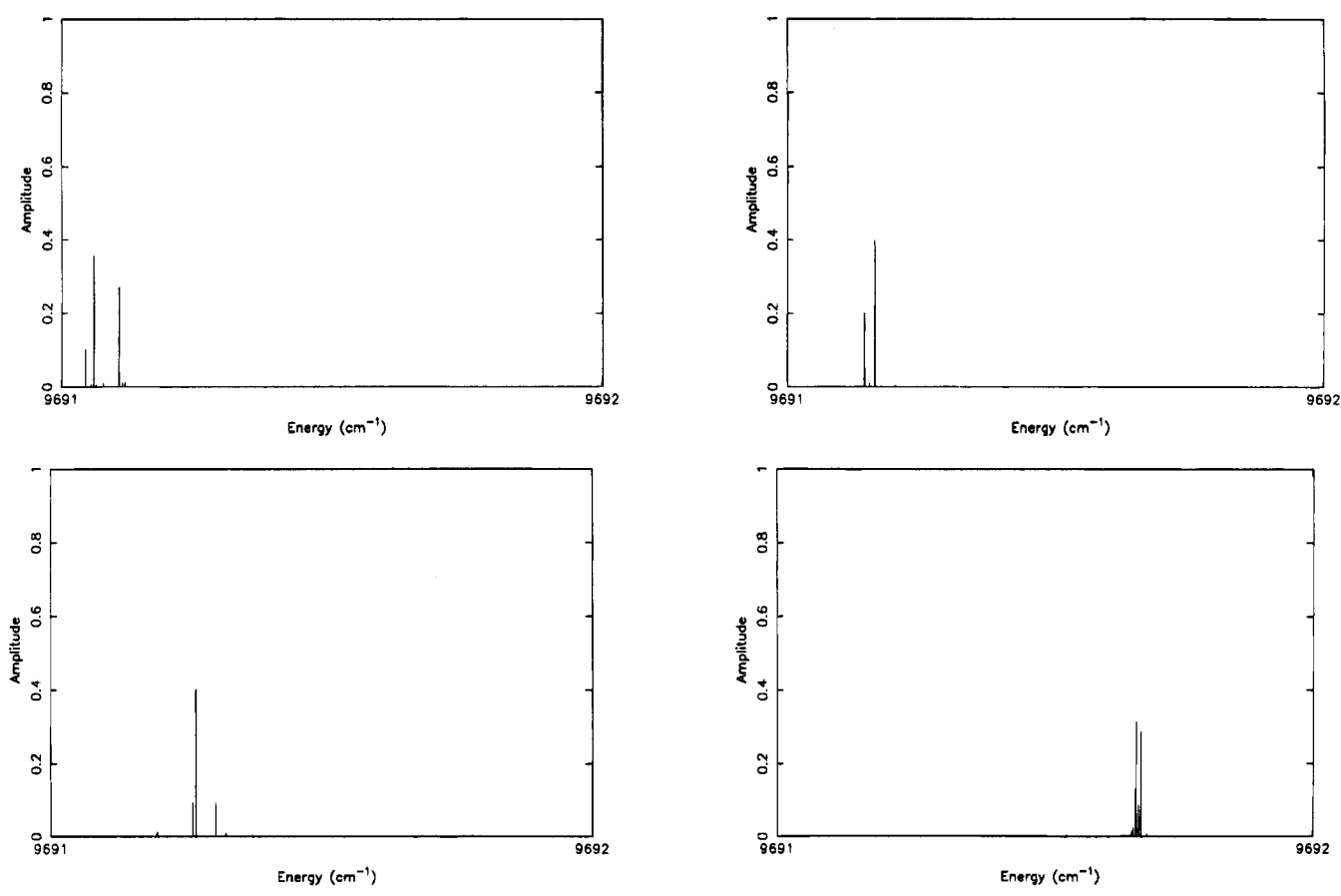


Figure 5. Spectra corresponding to the $3\nu_1$ band for CH₃CCH with different random realizations of the final tier of resonant states and quartic couplings.

TABLE 2: Statistical Properties of the Spectra in Figures 2 and 5

| 0.07 |
|------|
| 0.07 |
| 0.02 |
| 0.13 |
| 0.02 |
| |
| |

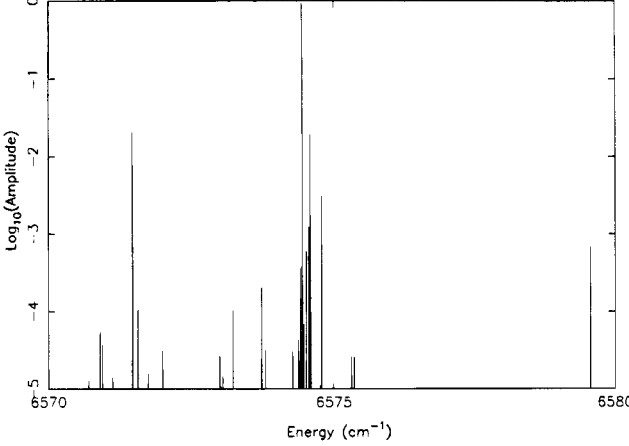


Figure 6. Spectrum typical of the $2\nu_1$ band with quartic couplings. Note the log scale for the ordinate.

IV. Discussion

4.1. $3v_1$. The first result to be considered is that the pure cubic Hamiltonian without the final tier does not result in any splitting of the individual spectral line. This result is not surprising since a near degeneracy of two or more states is needed, as a necessary though not sufficient condition, to

distribute the intensity of the bright state among two or more major peaks, and the density of states for that calculation is far lower than the real value. For this first result the density of states was approximately $2/\text{cm}^{-1}$, compared with the actual value of $150/\text{cm}^{-1}$. Similar results have been obtained for other calculations modeling the excitation of the acetylenic stretch in different molecules.² However, unlike the situation in *tert*-butylacetylene where the addition of an extra tier for the fundamental C-H stretch causes the single line to have a Lorentzian line shape,² the final tier (with a density of states appropriate to the $3\nu_1$ excitation energy in propyne) did not affect the spectrum. The total superexchange coupling of the bright state to the dense (phenomenological) tier was therefore so small that the states in the dense tier remained, in effect, uncoupled to the bright state.

Indeed, it has been shown previously² that while the presence of the total density of states in the tiers is a necessary condition for calculations to correctly simulate statistical or near-statistical IVR behavior, it is not a sufficient condition. Equally important is the correct description of the initial tiers as they govern the overall decay. It may be recalled that the lifetimes of various different initial states can be inferred from the analysis of only a few initial tiers. Here, the above mentioned results regarding the spectrum indicate that a correct description of the IVR of this bright state (at a higher energy than the states previously analyzed) requires the inclusion of terms higher than cubic in the Hamiltonian. In this way the superexchange matrix element to the states separated by a large distance in tier space will be larger. The next higher order of coupling beyond cubic consists of the quartic terms in the Hamiltonian. The procedure used to include such terms was described in a previous section. We note that the basis set initially used for the cubic couplings remains the same when the quartic couplings are introduced. The states in tier n that can be coupled to states in tiers n + 2 via terms of the type $q_iq_jq_kq_l$ are assigned an off-diagonal matrix element.

The importance of including quartic couplings for intramolecular dynamics of overtone states was observed previously by Zhang and Marcus.¹⁵ We next sketch how the inclusion of the quartic terms in the Hamiltonian can significantly increase the total coupling of overtone bright state. If the couplings are limited to third order, then the coupling between the bright state and the first tier is similar for v_1 , $2v_1$, and $3v_1$ since the *only* cubic coupling terms possible will annihilate one quantum of ν_1 (which is the highest energy oscillator) and create two others such that $v_1 \approx v_i + v_j$. The matrix elements that couple the bright state to the first tier for the fundamental as compared to the different overtone bands differ by a small multiplicative constant, due to the selection rules for harmonic oscillator wave functions. However, the number of states in the first tier and the approximate detuning of those states is roughly independent of whether the bright state is the fundamental band or an overtone. Consideration of higher order couplings modifies this picture. For the overtone states, application of the $q_iq_iq_iq_k$ and $q_iq_iq_iq_kq_l$ type of operators upon the bright state creates the additional couplings of fourth and fifth order, respectively, since more than one quantum in the initially excited state is available for annihilation. These quartic and quintic couplings have no effect on the bright state in the fundamental band, but their presence in the overtone bands significantly increases the overall coupling of the bright state to the bath and increases, thereby, also the superexchange matrix elements to the dense tier of states since, at the higher energies, states with some negative $\Delta \nu$'s can be coupled. These facts describe one role for quartic couplings in the calculations attempted for states at higher energies. Although a realistic modeling of the fundamentals in other molecules was possible when only the cubic couplings were included, 1,2 the present results show that, when higher energy states are considered, the use of only the cubic couplings underestimates the superexchange coupling of the bright state to the states in distant tiers. The increasing importance with energy of such higher order couplings or, in other words, the poorer pure cubic coupling picture of IVR is, therefore, indicated.

We consider next the small peaks that appear detuned to a relatively larger extent in energy in the spectra upon the addition of these quartic couplings. Upon the addition of the quartic constants, the spectrum dominated by a single peak splits to form some small peaks over a large energy window with most of the amplitude still being in the main peak. This result signifies that the coupling of the bright state to the states in the initial tiers has increased. As mentioned earlier, it is these couplings that control the total coupling of the bright state with the near-degenerate states that are separated in phase space. That the addition of the quartic couplings significantly increases this superexchange coupling is measured directly when a final tier of states is added along with the quartic couplings. Unlike the previous result, where without quartic terms the final tier made no difference, this time the single peak splits into a few peaks (Figures 2 and 5). The small peaks are due to the direct (and weak) coupling of the bright state with states in the initial tiers that are usually highly detuned. Experimentally these peaks have not been identified, since they appear on a energy scale greater than the scale investigated experimentally, $1-2 \text{ cm}^{-1}$, and their calculated intensity is small. Such small peaks in the wings have also been identified in calculations and discussed by Gruebele and co-workers.¹⁶

Although the approximations inherent in the present model calculations preclude a one-to-one correspondence of the peaks in the experimental and theoretical spectra, there is a qualitative similarity between them, both in the number of peaks and in the approximate energy range (0.1 cm⁻¹) over which they appear. The autocorrelation function shows a lifetime on the order of 300 ps. The mechanism that governs the physical process is again a vibrational superexchange coupling mechanism. This long smooth decay in Figure 4 is typical of the calculated relaxation of acetylenic stretches even though recurrences are not precluded. It may be recalled that one of the features of the acetylenic C-H stretch fundamentals and overtones was the absence of any direct low-order resonance.1,2 The states in the initial tiers were mostly all off-resonant and provided a virtual state mechanism (superexchange) for transition into the resonant states that were well separated in the phase (or quantum number) space of the molecule.

4.2. Other Spectral Bands. Due to the smaller density of available states at the given energy, the calculated spectra are mainly dominated by a single peak with some small daughter peaks arising due to quartic couplings. The final tier of states does not play a major role in the IVR. This IVR is not statistical and may be considered at the beginning of the intermediate stage. The results for the $\nu_1 + 2\nu_6$ band are not adequately treated by the present formulation, which should be regarded as a first step. For this band, and for $3\nu_1$, a more elaborate treatment would omit the x_{ij} terms and use, instead, a more elaborate force field and, perhaps, include vibration—rotation couplings.

V. Conclusion

We have calculated the spectral features of the first and second overtones of the acetylenic C-H stretch in propyne that arise from the anharmonic coupling between harmonic zeroth-order states. The energy and the couplings of the basis states are calculated from an empirical potential energy function.

We find that due to a lack of direct Fermi resonances, the C-H stretch decays into the dark vibrational states by utilizing the low-order off-resonant states that are available. Our results are qualitatively similar to the experimental ones. We show that the inclusion in the potential of terms higher than cubic is necessary for a correct representation of the spectrum. The calculations show that the initial couplings of the two bright states are both off-resonant in nature and provide the virtual couplings to available near-resonant states. Upon the inclusion of a final tier of states with the appropriate density of states, we find that the first overtone remains spectrally pure with one dominant component, whereas the second overtone spectrum consists of a few major components due to the availability of a higher density of states. In a temporal description, the presence of a higher density of states in the second overtone allows for the initially excited state to decay statistically, whereas the initial excitation remains more localized in the first overtone.

Acknowledgments. It is a pleasure to acknowledge the many insightful contributions of a friend and colleague, Stuart Rice, and to dedicate this article to him. This work is supported in part by the Caltech-JPL CRAY Supercomputing project. The calculations described here have been performed on the JPL-CRAY Y-MP2E/232. We thank Xueyu Song for useful discussions and are pleased to acknowledge the financial support of the National Science Foundation.

References and Notes

- Stuchebrukhov, A. A.; Marcus, R. A. J. Chem. Phys. 1993, 98, 6044.
- (2) Stuchebrukhov, A. A.; Mehta A.; Marcus, R. A. J. Phys. Chem. 1993, 97, 12491.

- (3) Kerstel, E. R. Th.; Lehmann, K. K.; Mentel, T. F.; Pate, B. H.; Scoles, G. J. Phys. Chem. 1991, 95, 8282. Gambogi, J. E.; L'Esperance, R. P.; Lehmann, K. K.; Pate, B. H.; Scoles, G. J. Chem. Phys. 1993, 98, 1116.
- (4) Gambogi, J. E.; Kerstel, E. R. Th.; Lehmann, K. K.; Scoles, G. J. Chem. Phys. 1994, 100, 2612. Gambogi, J. E.; Lehmann, K. K.; Timmermans, J. H.; Scoles, G. Abstracts of Papers, American Chemical Society, 1994, 207, 115-PHYS. Gambogi, J. E.; Timmermans, J. H.; Lehmann, K. K.; Scoles, G. J. Chem. Phys. 1993, 99, 9314.
- (5) Go, J. S.; Cronin, T. J.; Perry, D. S. Chem. Phys. 1993, 175, 127. (6) Herzberg, G. Infrared and Raman Spectra; D. van Nostrand: New York, 1945.
- (7) Hoy, A. R.; Mills, I. M.; Strey, G. Mol. Phys. 1972, 24, 1265.
 (8) Gaw, J. F.; Willetts, A.; Green, W. H.; Handy, N. C. In Advances in Molecular Vibrations and Collision Dynamics, Bowman, J. M., Ed.; JAI Press: Greenwich, CT, 1990.
- (9) Duncan, J. L.; McKean, D. C.; Nivellini, G. D. J. Mol. Struct. 1976, 32, 255.

- (10) Allen, W. D.; Yamaguchi, Y.; Császár, A. G.; Clabo, D. A., Jr.; Remington, R. B.; Schaefer, H. F., III. Chem. Phys. 1990, 145, 427.
 - (11) Challacombe, M.; Cioslowski, J. J. Chem. Phys. 1991, 95, 1064.
 - (12) Kondo, S.; Koga, Y.; Nakanaga, T. J. Chem. Phys. 1984, 81, 1951.
- (13) Frisch, M. J.; Trucks, G. W.; Head-Gordon, M.; Gill, P. M. W.; Wong, M. W.; Foresman, J. B.; Johnson, B. G.; Schlegel, H. B.; Robb, M. A.; Replogle, E. S.; Gomperts, R.; Andres, J. L.; Raghavachari, K.; Binkley, J. S.; Gonzalez, C.; Martin, R. L.; Fox, D. J.; Defrees, D. J.; Baker, J.; Stewart, J. J. P.; Pople, J. A. Gaussian 92, Revision D.2; Gaussian, Inc.: Pittsburgh, PA, 1992.
 - (14) Lawrance, W. D.; Knight, A. E. W. J. Phys. Chem. 1985, 89, 917.
 - (15) Zhang, Y.-F.; Marcus, R. A. J. Chem. Phys. 1992, 97, 5283.
 - (16) Gruebele, M. Private communication and preprint.

JP942667B